

## HIGH $k_T$ MESON PRODUCTION: A DIFFERENT WAY TO PROBE HADRON STRUCTURE<sup>a</sup>

CARL E. CARLSON

*Nuclear and Particle Theory Group, Physics Department,  
College of William and Mary, Williamsburg, VA 23187-8795*

Hard, or high transverse momentum, pion photoproduction can be a tool for probing the parton structure of the beam and target. We discuss the perturbative and soft processes that contribute, and show how regions where perturbative processes dominate can give us the parton structure information. Polarized initial states are needed to get information on polarization distributions. Current polarization asymmetry data is mostly in the soft region. However, with the proposed EPIC machine parameters, determining the polarized gluon distribution using hard pion photoproduction appears quite feasible.

### 1 Semi-Exclusive Processes as Probes of Hadron Structure

Information about hadron structure, in the form of distribution functions or quark wave functions, classically comes from deep inelastic scattering, Drell-Yan processes, or coincident electroproduction<sup>1</sup>. What we shall study here is the possibility of getting the same kind of information from photoproduction of hard, which means high transverse momentum, pions or non-coincident electroproduction of the same<sup>2,3,4,5,6,7</sup>. The production can proceed by a number of processes, including direct pion production, direct photon interactions followed by parton fragmentation, resolved photon processes, and soft processes. The first of these, direct pion production can also be called short-distance or isolated pion production. In the following, we will discuss how the first two of these processes can give hadronic distribution function and wave function information. Information can also come from resolved photon processes in the right circumstances, but we shall not pursue them here. Soft processes are from the present viewpoint an annoyance, but one we need to discuss and estimate the size of. All the processes will be defined and discussed below.

To begin being more explicit, the semi-exclusive process we will discuss is

$$\gamma + A \rightarrow M + X, \quad (1)$$

where  $A$  is the target and  $M$  is a meson, here the pion. The process is perturbative because of the high transverse momentum of the pion, not because of the high  $Q^2$  of the photon. Our considerations will also apply to electroproduction,

<sup>a</sup>Invited talk given at the Electron Polarized Ion Collider Workshop (EPIC99), at the Indiana University Cyclotron Facility, Bloomington, Indiana, USA, 8–11 April 1999

$$e + A \rightarrow M + X \quad (2)$$

if the final electron is not seen. In such a case, the exchanged photon is nearly on shell, and we use the Weizäcker-Williams equivalent photon approximation<sup>8</sup> to relate the electron and photon cross sections,

$$d\sigma(eA \rightarrow MX) = \int dE_\gamma N(E_\gamma) d\sigma(\gamma A \rightarrow MX), \quad (3)$$

where the number distribution of photons accompanying the electron is a well known function.

In the following section, we will describe the subprocesses that contribute to hard pion production, and in the subsequent section display some results. Section 4 will be a short summary.

## 2 The Subprocesses

### 2.1 At the Highest $k_T$

At the highest possible transverse momenta, observed pions are directly produced at short range via a perturbative QCD (pQCD) calculable process<sup>4,5,6,7</sup>. Two out of four lowest order diagrams are shown Fig. 1. The pion produced this way is kinematically isolated rather than part of a jet, and may be seen either by making an isolated pion cut or by having some faith in the calculation and going to a kinematic region where this process dominates the others. Although this process is higher twist, at the highest transverse momenta its cross section falls less quickly than that of the competition, and we will show plots indicating the kinematics where it can be observed.

The subprocess cross section for direct or short-distance pion production is

$$\frac{d\hat{\sigma}}{dt}(\gamma q \rightarrow \pi^\pm q') = \frac{128\pi^2\alpha\alpha_s^2}{27(-t)\hat{s}^2} I_\pi^2 \left( \frac{e_q}{\hat{s}} + \frac{e'_q}{\hat{u}} \right) [\hat{s}^2 + \hat{u}^2 + \lambda h(\hat{s}^2 - \hat{u}^2)], \quad (4)$$

where  $\hat{s}$ ,  $\hat{t} = t$ , and  $\hat{u}$  are the subprocess Mandelstam variables;  $\lambda$  and  $h$  are the helicities of the photon and target quark, respectively; and  $I_\pi$  is an integral related to the pion wave function at the origin in coordinate space,

$$I_\pi = \int \frac{dy_1}{y_1} \phi_\pi(y_1, \mu^2). \quad (5)$$

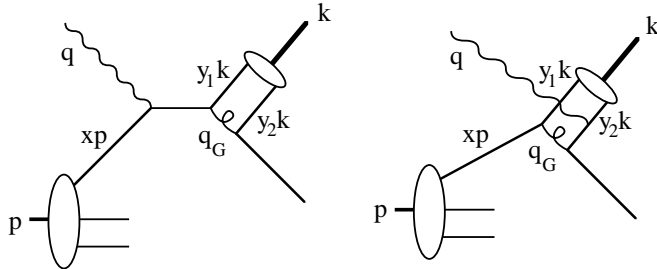


Figure 1: Direct pion production. The pion is produced in a short distance perturbatively calculated process, not by fragmentation of an outgoing parton. Thus this pion is kinematically isolated, and not part of a jet. Direct pion production gets important at very high transverse momentum because the pion does not have to share the available momentum with any other particles going in its direction.

In the last equation,  $\phi_\pi$  is the distribution amplitude of the pion, and describes the quark-antiquark part of the pion as a parallel moving pair with momentum fractions  $y_i$ . It is normalized through the rate for  $\pi^\pm \rightarrow \mu\nu$ , and for example,

$$\phi_\pi = \frac{f_\pi}{2\sqrt{3}} 6y_1(1-y_1) \quad (6)$$

for the distribution amplitude called “asymptotic” and for  $f_\pi \approx 93$  MeV. Overall, of course,

$$\frac{d\sigma}{dx dt}(\gamma A \rightarrow \pi X) = \sum_q G_{q/A}(x, \mu^2) \frac{d\hat{\sigma}}{dt}(\gamma q \rightarrow \pi^\pm q'), \quad (7)$$

where  $G_{q/A}(x, \mu^2)$  is the number distribution for quarks of flavor  $q$  in target  $A$  with momentum fraction  $x$  at renormalization scale  $\mu$ .

Let us note a number of points about direct pion production.

- For the photoproduction case, at least, the momentum fraction of the struck quark is determined from experimental observables. This is like the situation in deep inelastic scattering, where the experimenter can measure  $x \equiv Q^2/2m_N\nu$  and the theorist can prove that this  $x$  is the same as the momentum fraction of the struck quark, for high  $Q$  and  $\nu$ . For the present case, define the momenta

$$\gamma(q) + A(p) \rightarrow \pi(k) + X, \quad (8)$$

and then the Mandelstam variables for the overall process,

$$s = (p + q)^2; \quad t = (q - k)^2; \quad \text{and} \quad u = (p - k)^2. \quad (9)$$

Each of the Mandelstam variables is an observable, and the ratio

$$x = \frac{-t}{s + u} \quad (10)$$

is the momentum fraction of the struck quark. We will let the reader prove this.

- The gluon involved in direct pion production is well off shell. We will illustrate this by comparison to the pion electromagnetic form factor. For the gluon in Fig. 1(right),

$$q_G^2 = (xp - y_1 k)^2 = y_1 x u. \quad (11)$$

(The gluon in Fig. 1(left) is farther off shell.) To get a number, take  $E_\gamma = 100$  GeV and  $90^\circ$  in the center of mass. Then  $u \approx -95$  GeV<sup>2</sup>, and using  $\langle y_1 \rangle \approx 1/3$  and  $x \approx 1/2$  gives

$$\langle q_G^2 \rangle \approx -15 \text{ GeV}^2. \quad (12)$$

In a calculation of  $F_\pi$ ,

$$\langle q_G^2 \rangle = \langle y_1 y_2' \rangle q^2 \approx \frac{1}{9} q^2, \quad (13)$$

where  $y_1$  and  $y_2'$  are the momentum fractions, in the incoming and outgoing pion, of the quark that does not absorb the photon. Hence to match the above direct pion production kinematics requires measuring  $F_\pi$  at a momentum transfer  $|q^2| = 135$  GeV<sup>2</sup>. We come much closer to asymptopia in direct pion production than in a thinkable pion form factor measurement!

- Without polarization, we can measure  $I_\pi$ , given enough trust in the other parts of the calculation. This  $I_\pi$  is precisely the same as the  $I_\pi$  in both  $\gamma^* \gamma \rightarrow \pi^0$  (which is measured in  $ee \rightarrow ee\pi^0$ ) and  $e\pi^\pm \rightarrow e\pi^\pm$  (which gives the pion form factor  $F_\pi$ ). Presently, the experimental results for  $\gamma^* \gamma \rightarrow \pi^0$  agree with the theoretical results using the asymptotic distribution amplitude mentioned earlier, but the results for  $F_\pi$  disagree with the same. Thus there is room for a third process in measuring  $I_\pi$ .

- We also have polarization sensitivity in direct pion production. For  $\pi^+$  production at high  $x$ ,

$$A_{LL} \equiv \frac{\sigma_{R+} - \sigma_{L+}}{\sigma_{R+} + \sigma_{L+}} = \frac{s^2 - u^2}{s^2 + u^2} \frac{\Delta u(x)}{u(x)} \quad (14)$$

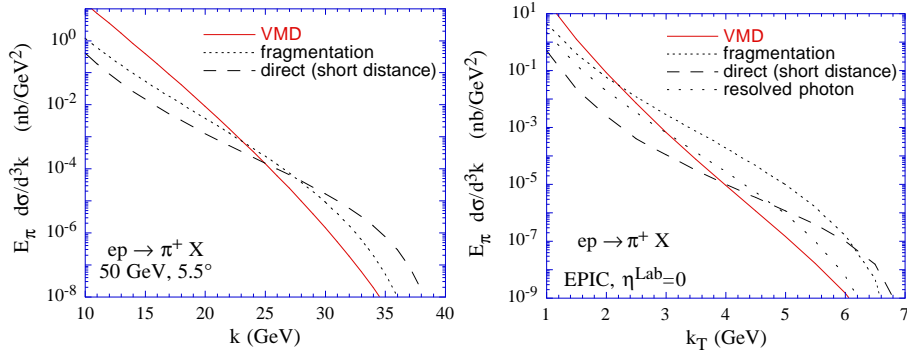


Figure 2: Calculated contributions to the cross section for  $ep \rightarrow \pi^+ X$ . Results for SLAC energies with the pion emerging at  $5.5^\circ$  in the lab are shown on the left. Results for projected EPIC kinematics, 4 GeV electrons colliding with 40 GeV protons, with pions emerging at  $90^\circ$  (or rapidity  $\eta$  being 0) in the lab are shown on the right. The direct process should be quite important at SLAC (or HERMES), once we have enough transverse momentum to escape the ‘soft’ region; EPIC has a long window where the fragmentation process dominates.

where  $R$  and  $L$  refer to the polarization of the photon, and  $+$  refers to the target, say a proton, polarization. Also, inside a  $+$  helicity proton the quarks could have either helicity, and

$$\Delta u(x) \equiv u_+(x) - u_-(x). \quad (15)$$

The large  $x$  behavior of both  $d(x)/u(x)$  and  $\Delta d(x)/\Delta u(x)$  are of current interest. Most fits to the data have the down quarks disappearing relative to the up quarks at high  $x$ , in contrast to pQCD which has definite non-zero predictions for both of the ratios in the previous sentence. Recent improved work on extracting neutron data from deuteron targets, has tended to support the pQCD predictions<sup>9</sup>.

There is some data already on  $A_{LL}$ <sup>10</sup>, from SLAC End Station A, which we shall show when we have discussed some of the other processes that can produce pions. However, the reader who has gotten this far should get to see plots that show, at least by calculation, that there is a non-empty region where direct or short-range pion production can be seen. To this end, Fig. 2 shows the differential cross section for high transverse momentum  $\pi^+$  electroproduction for two different kinematics. The leftmost figure is for a SLAC energy, 50 GeV incoming electrons, with the pion emerging at  $5.5^\circ$  in the lab. It shows that above about 27 GeV total pion momentum or 2.6 GeV transverse momentum,

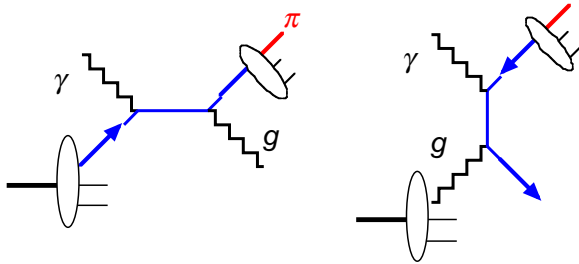


Figure 3: The fragmentation process. Pions are produced by fragmentation of partons at long distances from the primary interaction region. The Compton process is on the left; the pion could come from either quark or gluon fragmentation. Quark-gluon fusion is on the right.

direct (short distance, isolated) pion production exceeds its competition. The rightmost plot is tuned to what I understand is a discussed possibility for EPIC, namely 4 GeV electrons colliding with 40 GeV protons, with the pions emerging at  $90^\circ$  in the lab. Again, the direct pion process dominates at high enough momentum, although this time the crossover point is higher and the crossover cross section lower.

## 2.2 Moderate $k_T$

At moderate transverse momentum, the generally dominant process is still a direct interaction in the sense that the photon interacts directly with constituents of the target, but the pion is not produced directly at short range but rather at long distances by fragmentation of some parton<sup>2,3,6</sup>. Many authors refer to this as the direct process; others of us are in the habit of calling it the fragmentation process. The main subprocesses are called the Compton process and photon-gluon fusion, and one example of each is shown in Fig. 3.

A key feature of hard pion photoproduction in vis the fragmentation process is that the target gluons are involved in lowest order. This stands in contrast to deep inelastic scattering, Drell-Yan processes, or coincident electroproduction, where target gluons affect the cross sections only in next-to-leading order (NLO). These NLO effects can be significant enough with precise data to give a good determination of the gluon distribution, and indeed the unpolarized gluon distribution  $g(x)$  has been determined this way. However, for the polarized distribution  $\Delta g(x)$ , the situation is unsettled. Fig. 4 shows a number of different  $\Delta g(x)$ , normalized to a common  $g(x)$ , that have been derived from

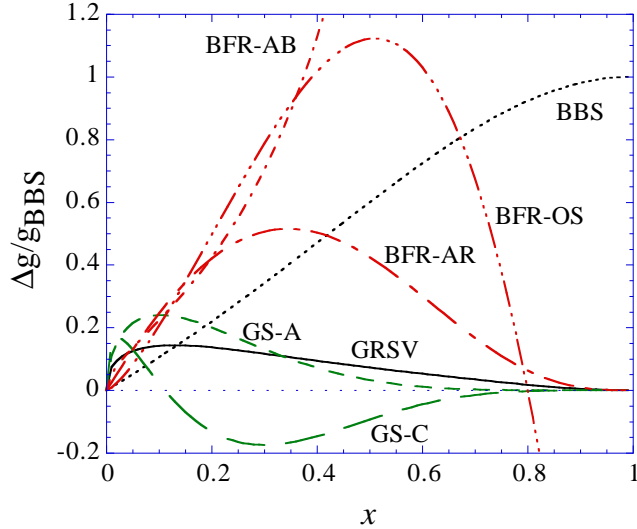


Figure 4: Possible polarized gluon distributions, all divided by the same unpolarized distribution. Most of these are derived from NLO effects on data and all are claimed to lead to agreement with the data. References are BBS<sup>21</sup>; BFR<sup>22</sup>; GRSV<sup>23</sup>; and GS<sup>24</sup>.

analyses of NLO effects and that all purport to fit the data. There is clearly need for additional information, and photon gluon fusion could supply it. Photon gluon fusion often gives 30–50% of the cross section for the fragmentation process, and the polarization asymmetry is as large as can be in magnitude,

$$\hat{A}_{LL}(\gamma g \rightarrow q\bar{q}) = -100\%. \quad (16)$$

Typically for the Compton process,  $\hat{A}_{LL}(\gamma q \rightarrow gq) \approx 1/2$ . To use the fragmentation process we need to have a significant region where that process dominates, and we need to know the sensitivity of the measured polarization asymmetry to the different plausible models for  $\Delta g(x)$ . EPIC is the right energy to give a significant region where the fragmentation process dominates, as may be seen from the right hand part of Fig. 2. The sensitivity is also good, but we shall put off showing the  $\hat{A}_{LL}$  plots until we discuss the soft processes.

We should also note that the NLO calculations for the fragmentation process have been done also for the polarized case, though our plots are based on LO. For direct pion production, NLO calculations are not presently completed.

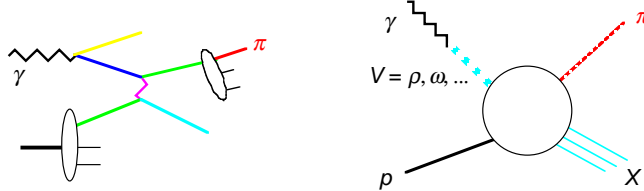


Figure 5: Resolved photon process (left) and vector meson dominated process (right).

### 2.3 Resolved Photon Processes

The photon may split into hadronic matter before interacting with the target. If it splits into a quark anti-quark pair that are close together, the splitting can be modeled perturbatively or quasi-perturbatively, and we call it a resolved photon process. Perturbative QCD calculations of the entire process can ensue, and a typical diagram is shown in the left hand part of Fig. 5. Though resolved photon processes are crucial at HERA energies, they are never dominant at energies under discussion here, and we say no more about them.

### 2.4 Soft Processes

This is the totally non-perturbative part of the calculation, whose size can be estimated by connecting it to hadronic cross sections. The photon may turn into hadronic matter, such as  $\gamma \rightarrow q\bar{q} + \dots$  with a wide spatial separation. It can be represented as photons turning into vector mesons. A picture is shown on the right of Fig. 5.

We want a reliable approximation to the non-perturbative cross section so we can say where perturbative contributions dominate and where they do not. Briefly, what we<sup>11</sup> have done to get such an approximation is to start with the cross section, given as

$$d\sigma(\gamma A \rightarrow \pi X) = \sum_V \frac{\alpha}{\alpha_V} d\sigma(V + A \rightarrow \pi X) + \text{non - VMD}, \quad (17)$$

where the sum is over vector mesons  $V$ ,  $\alpha = e^2/4\pi$ , and  $\alpha_V = f_V^2/4\pi$ , with the photon-vector meson vertex in Fig. 5 (right side) given as  $em_V^2/f_V$ . We can get, for example,  $f_\rho$  from the decay  $\rho \rightarrow e^+e^-$ .

Contributions from the  $\rho'$  and other excited  $\rho$  mesons are compensated changing  $\alpha_V$  into  $\alpha_V^{eff}$ , which is about 20% higher<sup>12</sup>. Including the  $\omega$  and  $\phi$



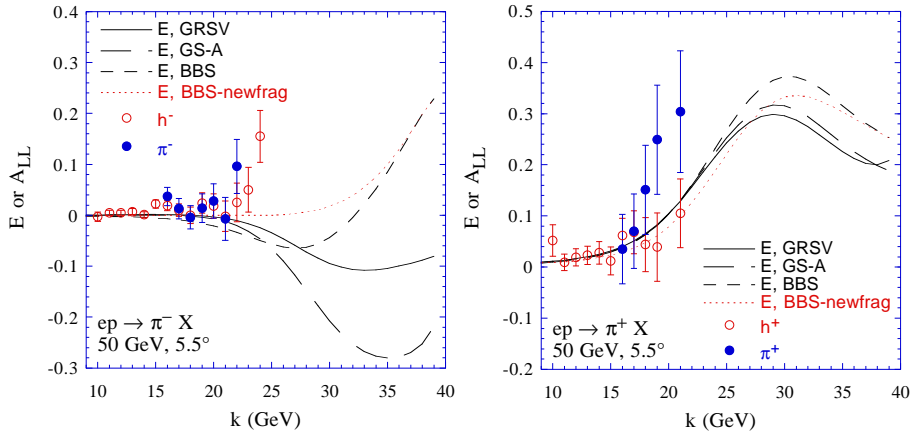


Figure 6: Longitudinal polarization asymmetries for  $\pi^\pm$  production at  $5.5^\circ$  in the lab off proton targets at SLAC energies. The calculations are shown for three different polarized parton distributions<sup>21,23,24</sup> and, for the BBS case, one non-standard fragmentation function set<sup>11</sup>. Much of the data is in the region where the soft processes are dominant, and the data is consistent with little polarization sensitivity in the soft region. The  $\pi^+$ , however, may be showing polarization asymmetry from fragmentation or direct pion production processes coming in at the higher momenta.

increases the result by 33%, according to SU(3). Now we “just” need the cross section for  $\rho^0 A \rightarrow \pi^+ X$ . Lacking direct data, we approximate it by

$$d\sigma(\rho^0 p \rightarrow \pi^+ X) \approx d\sigma(\pi^+ p \rightarrow \pi^0 X) \approx 1.3d\sigma(\pi^+ p \rightarrow \pi^- X). \quad (18)$$

Part of this sequence is backed up by data of O’Neill *et al.*<sup>13</sup>. Then we used data and data reductions of Bosetti *et al.*<sup>14</sup> and Beier *et al.*<sup>15</sup> to get a parameterized fit to the last cross section. One can compare what we did to the Regge fit for soft processes of T. Sjöstrand *et al.*, which is implemented in PYTHIA<sup>16</sup>.

We took the soft processes to be polarization insensitive. This agrees with a recent Regge analysis of Manayenkoy<sup>17</sup>.

### 3 Results

Results for the unpolarized cross section have already been displayed in Fig. 2. The soft VMD process is the most important out to transverse momenta of about 2 GeV. Above this, at SLAC energies, one almost immediately enters a region where direct pion production is the main process. At planned EPIC

energies, however, there is a long region where the fragmentation process dominates, and this can be of use in studying  $\Delta g$ .

Most interesting may be the calculations of  $E$  or  $A_{LL}$ , and together with the recent data from SLAC. (Here  $E$  is just old notation for  $A_{LL}$ . Barker *et al.*<sup>18</sup> in 1975 listed all measurable asymmetries in pion photoproduction and what we call  $A_{LL}$  was the fifth on their list—and  $E$  is the fifth letter of the alphabet.) Fig. 6 shows the calculated  $A_{LL}$  for both  $\pi^-$  and  $\pi^+$  off proton targets for three different parton distribution models. Although the fragmentation process is not the crucial one here, we should mention that mostly we used our own fragmentation functions<sup>4</sup>, and that the results using BKK<sup>19</sup> are not very different. Neither set of fragmentation functions agrees well with the most recent HERMES data<sup>20</sup> for unfavored vs. favored fragmentation functions, and the one curve labeled “newfrag” is calculated with fragmentation functions that agree better that data (assuming that data should be explained by simple fragmentation alone).

Below about 20 GeV total pion momentum, the soft process dominates and the data is indeed well described by supposing the soft processes have no polarization asymmetry. Above that, the asymmetry is calculated in pQCD, and the difference among the results for the different sets of parton distributions is quite large for the  $\pi^-$ .

The data of Anthony *et al.*<sup>10</sup> is also shown. Presently most, though not all, of the data is in the region where the soft processes dominate. The data is already interesting. Further data at even higher pion momenta would be even more interesting, especially for the  $\pi^-$ . Large momentum corresponds to  $x \rightarrow 1$  for the struck quark, and pQCD predicts that the quarks are 100% polarized in this limit. Only the parton distributions labeled “BBS” are in tune with the pQCD prediction, and they for large momentum predict even a different sign for  $A_{LL}$  for the  $\pi^-$ . The experiment also has data for deuteron targets, and the calculated results plotted with the data for this case may be examined in<sup>11</sup>.

Regarding EPIC, there is the long region where the fragmentation process dominates, and we would like to know how sensitive the possible measurements of  $A_{LL}$  are to the different models for  $\Delta g$ . To this end, we present in Fig. 7 the results for  $A_{LL}$  for one set of quark distributions and 5 different distributions for  $\Delta g$ . The quark distributions and unpolarized gluon distribution in each case are those of GRSV. There are 6 curves on each figure. One of them is a benchmark, which was calculated with  $\Delta g$  set to zero. The other curves use the  $\Delta g$  from the indicated distribution. There is a fair spread in the results, especially for the  $\pi^-$  where photon-gluon fusion gives a larger fraction of the cross section. Thus, one could adjudicate among the polarized gluon

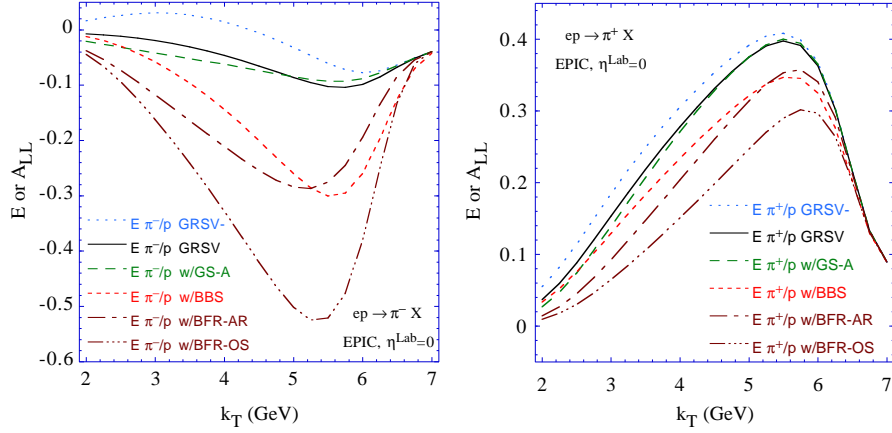


Figure 7: Polarization asymmetries for different  $\Delta g$ 's for projected EPIC energies, with  $\pi^\pm$  emerging at  $90^\circ$  or zero rapidity in the lab. Each figure has six curves. All use the same quark distributions, namely the ones from GRSV<sup>23</sup>. One curve (“GRSV-”) is purely benchmark, having the polarized gluon distribution  $\Delta g$  set to zero. The other five curves use five different model  $\Delta g$ <sup>21,22,23,24</sup>, as labeled, to show the potential effectiveness of this measurement for culling gluon polarization models.

distribution models.

## 4 Summary

Hard, meaning high transverse momentum, semiexclusive processes such as  $\gamma p \rightarrow \pi X$  provide a different way to probe parton distributions.

There are several perturbative processes that contribute, which we have called the direct (or isolated or short distance) pion production process, the fragmentation process, and the resolved photon process. All are calculable. They give us new ways to measure aspects of the pion wave function, and quark and gluon distributions, especially  $\Delta q$  and  $\Delta g$ . The soft processes can be estimated and avoided if the transverse momentum is greater than about 2 GeV. EPIC is projected to have a wide window in which the fragmentation process dominates, which should make it excellent, in particular, for measuring  $\Delta g$ .

## Acknowledgments

My work on this subject has been done with Andrei Afanasev, Chris Wahlquist, and A. B. Wakely and I thank them for pleasant collaborations. I have also benefited from talking to and reading the work of many authors and apologize to those I have not explicitly cited. I thank the NSF for support under grants PHY-9600415 and PHY-9900657.

## References

1. L. L. Frankfurt *et al.*, *Phys. Lett. B* **230**, 141 (1989); F. E. Close and R. G. Milner, *PRD* **44**, 3691 (1991); B. Adeva *et al.*, *Phys. Lett. B* **369**, 96 (1996).
2. D. De Florian and W. Vogelsang, *Phys. Rev. D* **57**, 4376 (1998); B. A. Kniehl, Talk at Ringberg Workshop, hep-ph/9709261; M. Stratmann and W. Vogelsang, Talk at Ringberg Workshop, hep-ph/9708243.
3. J. J. Peralta, A. P. Contogouris, B. Kamal and F. Lebessis, *Phys. Rev. D* **49**, 3148 (1994).
4. C. E. Carlson and A. B. Wakely, *Phys. Rev. D* **48**, 2000 (1993).
5. A. Afanasev, C. E. Carlson, and C. Wahlquist, *Phys. Lett. B* **398**, 393 (1997).
6. A. Afanasev, C. E. Carlson, and C. Wahlquist, *Phys. Rev. D* **58**, 054007 (1998).
7. S. J. Brodsky, M. Diehl, P. Hoyer, S. Peigne, *Phys. Lett. B* **449**, 306 (1999).
8. See for example the Appendix to S. J. Brodsky, T. Kinoshita, and H. Terazawa, *Phys. Rev. D* **4**, 1532 (1971).
9. W. Melnitchouk, J. Speth, and A. W. Thomas, *PLB* **435**, 420 (1998); W. Melnitchouk and J.C. Peng, *Phys. Lett. B* **400**, 220 (1997); W. Melnitchouk and A. W. Thomas, *Phys. Lett. B* **377**, 11 (1996); U. K. Yang and A. Bodek, *Phys. Rev. Lett.* **82**, 2467 (1999).
10. P. L. Anthony *et al.*, SLAC-PUB-8049 (1999); hep-ph/9902412.
11. A. Afanasev, C. E. Carlson, and C. Wahlquist, hep-th/9903493.
12. A. Pautz and G. Shaw, hep-ph/9710235.
13. L. H. O'Neill *et al.*, *Phys. Rev. D* **14**, 2878 (1976).
14. P. Bosetti *et al.*, *Nucl. Phys. B* **54**, 141 (1973).
15. E. Beier *et al.*, *Phys. Rev. D* **18**, 2235 (1978).
16. G. Schuler and T. Sjöstrand, *Nucl. Phys. B* **407**, 539 (1993); T. Sjöstrand, *J. Phys. G* **22**, 709 (1996). The physics described in these articles has been implemented as part of the PYTHIA event generation code. See T. Sjöstrand, *Comput. Phys. Commun.* **82**, 74 (1994).

17. S. I. Manayenkov, report DESY 99-016, hep-ph/9903405.
18. I.S. Barker, A. Donnachie, and J.K. Storrow, *Nucl. Phys. B* **95**, 347 (1975).
19. J. Binneweis, B. A. Kniehl, and G. Kramer, *Z. Phys. C* **65**, 471 (1995) and *Phys. Rev. D* **52**, 4947 (1995).
20. N. Makins, Proceedings of CEBAF Workshop on Physics and Instrumentation with 6-12 GeV Beams, ed. S. Dytman, H. Fenker, and P. Roos, JLab, Newport News, June 1998, p.97; Ph. Geiger, *Measurement of Fragmentation Functions at HERMES*, Ph. D. Thesis, Ruprecht-Karls-Universität, Heidelberg, 1998.
21. S. J. Brodsky, M. Burkardt, and I. Schmidt, *Nucl. Phys. B* **441**, 197 (1995).
22. R. D. Ball, S. Forte, and G. Ridolfi, *Phys. Lett. B* **378**, 255 (1996).
23. M. Glück, E. Reya, M. Stratmann, and W. Vogelsang, *Phys. Rev. D* **53**, 4775 (1996).
24. T. Gehrmann and W. J. Stirling, *Phys. Rev. D* **53**, 6100 (1996).